



DNA gyrase (GyrB)/topoisomerase IV (ParE) inhibitors: Synthesis and antibacterial activity

Stephen P. East^{a,*}, Clara Bantry White^a, Oliver Barker^a, Stephanie Barker^b, James Bennett^b, David Brown^b, E. Andrew Boyd^a, Christopher Brennan^a, Chandana Chowdhury^a, Ian Collins^b, Emmanuelle Convers-Reignier^a, Brian W. Dymock^a, Rowena Fletcher^b, David J. Haydon^b, Mihaly Gardiner^a, Stuart Hatcher^a, Peter Ingram^a, Paul Lancett^b, Paul Mortenson^a, Konstantinos Papadopoulos^a, Carol Smee^b, Helena B. Thomaidis-Brears^b, Heather Tye^a, James Workman^a, Lloyd G. Czaplowski^{b,*}

^a Evotec (UK) Ltd, Discovery Services, 114 Milton Park, Abingdon, Oxfordshire OX14 4SA, UK

^b Prolysis Ltd, Oxford University Begbroke Science Park, Sandy Lane, Yarnton, Oxfordshire OX5 1PF, UK

ARTICLE INFO

Article history:

Received 10 October 2008

Revised 24 November 2008

Accepted 26 November 2008

Available online 3 December 2008

Keywords:

Antibacterial

Gyrase

Imidazopyridine

Triazolopyridine

ABSTRACT

The synthesis and antibacterial activities of three chemotypes of DNA supercoiling inhibitors based on imidazolo[1,2-*a*]pyridine and [1,2,4]triazolo[1,5-*a*]pyridine scaffolds that target the ATPase subunits of DNA gyrase and topoisomerase IV (GyrB/ParE) is reported. The most potent scaffold was selected for optimization leading to a series with potent Gram-positive antibacterial activity and a low resistance frequency.

© 2008 Elsevier Ltd. All rights reserved.

The type II bacterial topoisomerases DNA gyrase and topoisomerase IV, which are responsible for the control of DNA topology and chromosome function, have been validated as a therapeutic drug target by members of the quinolone/fluoroquinolone class of antibacterial agents (e.g. gemifloxacin).¹ This particular class of compounds interact with the catalytic subunits of DNA gyrase (GyrA) and topoisomerase IV (ParC). The ATPase subunits of these enzymes GyrB and ParE have also been identified as the target for small molecule inhibitors (e.g. novobiocin), however, to date, issues surrounding resistance, toxicity and permeability of these inhibitors have limited their therapeutic use (Fig. 1).²

Recently, interest in identifying small molecule inhibitors of GyrB to overcome the liabilities of the existing compounds has intensified.^{3,4} Elucidation of protein–ligand structures of GyrB by X-ray crystallography^{5,6} has aided the search for new inhibitors and Tanitame et al.⁷ (e.g. pyrazole **1**), Mani et al.,⁸ Grossman et al.⁹ and Charifson et al. (e.g. benzimidazole **2**)¹⁰ have provided

examples of potent dual-targeting GyrB/ParE inhibitors which demonstrate good antibacterial activity (Fig. 2).

Encouraged by these disclosures, we explored a number of possible replacements for the benzimidazole core of **2**. We reasoned that it might be possible to find other 5,6-fused heterocyclic scaffolds that could provide different SAR and optimization opportunities as well as alternative ADME, pharmacology, toxicology and efficacy profiles. Our requirements for each new scaffold were to fix the 2-amino substituent as the ethylurea and one of the core substituents as the 3-pyridyl group. These proposals were docked into the ATP binding site of a GyrB model generated from the structure (PDB 1E11) deposited by Brino et al.⁵ We scrutinized our pro-

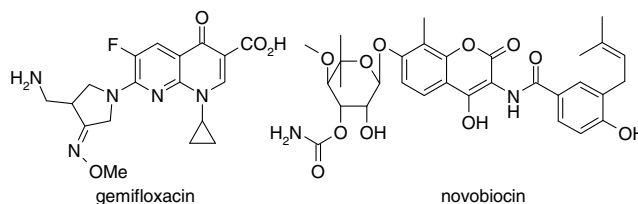


Figure 1. Gyrase inhibitors.

* Corresponding authors. Tel.: +44 (0) 1235 441735 (S.P. East), +44 (0) 1865 854700 (L.G. Czaplowski).

E-mail addresses: stephen.east@evotec.com (S.P. East), lloyd.czaplowski@prolysis.com (L.G. Czaplowski).

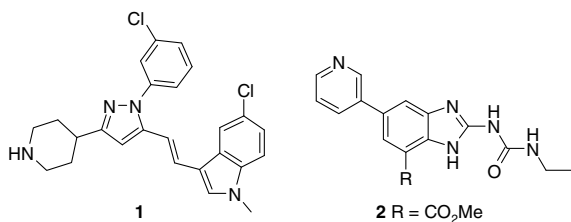


Figure 2. Reported GyrB/ParE inhibitors.

posals according to the interactions that they made with the enzyme and the three scaffolds that were the most appealing as predicted by our model were the imidazo[1,2-*a*]pyridine and the two isomeric [1,2,4]triazolo[1,5-*a*]pyridines (Fig. 3). The key binding interactions according to our docking studies are illustrated for triazolopyridine **5**. The scaffold and urea interactions have been previously described by Charifson et al.,¹⁰ but the interaction between the 3-pyridyl substituent and Arg136, which they described as a H-bond, appears more likely to be a π -stacking interaction in our model.

To test our modeling hypothesis we prepared **3**, **4** and **5**. Compounds **3** and **4** were synthesised from a common bipyridyl amine intermediate **7**, which was accessed via a modified Suzuki reaction using 2-amino-4-chloropyridine **6**¹¹ and 3-pyridyl boronic acid. The imidazopyridine **3** was synthesized in six steps from intermediate **7**. First, **7** was converted to the corresponding tosylate using *p*-toluenesulfonyl chloride and this was followed by alkylation with iodoacetamide to give **8**. Cyclisation to provide the imidazopyridine scaffold¹² was effected by treatment of **8** with trifluoroacetic anhydride. After removal of the trifluoroacetate group using potassium carbonate and methanol, compound **9** was obtained. Attempts to form the urea by reaction of **9** with ethyl isocyanate were unsuccessful. Instead we resorted to a two-step protocol with phenyl chloroformate to provide the phenyl carbamate followed by reaction with ethylamine to give **3**, albeit in very low yield.^{13,14}

To obtain the triazolopyridine **4**, compound **7** was treated with ethoxycarbonylisothiocyanate to provide thiourea **10** which was reacted with hydroxylamine according to the procedure described by Nettekoven et al.¹⁵ to give the triazolopyridine (not shown) which was then treated with ethyl isocyanate to give compound **4** in moderate overall yield. Triazolopyridine **5** was prepared via an analogous route to **4** but using 2-amino-5-iodopyridine as the starting material.

The compounds were screened in GyrB and ParE ATPase assays (*Escherichia coli*)¹⁶ and minimum inhibitory concentrations (MICs)¹⁷ were determined against Gram-positive (*Staphylococcus aureus* ATCC 29213 and *Enterococcus faecalis* ATCC 29212) and Gram-negative (*E. coli* N43 efflux pump mutant) bacterial strains (Table 1).¹⁸

The imidazopyridine **3** was the most active of the compounds tested with a sub-micromolar IC₅₀ against GyrB and it demon-

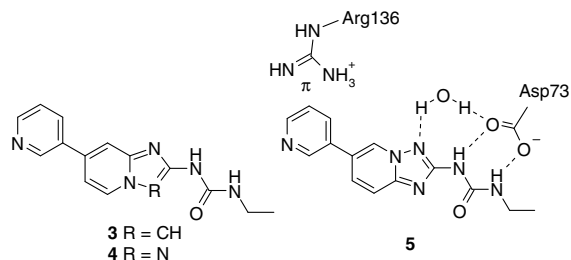


Figure 3. Proposed GyrB/ParE inhibitors.

Table 1
GyrB and ParE inhibitory activity and MICs

Compound	GyrB IC ₅₀ (μM)	ParE IC ₅₀ (μM)	MIC (μg/ml)		
			<i>S. aureus</i>	<i>E. faecalis</i>	<i>E. coli</i>
Novobiocin	0.03	1.32	0.125	8	8
2	0.009	3.5	0.25	0.125	1
2 ^a	<0.004	0.035	0.063	nd	nd
3	0.39	nd	32	32	32
4	2.68	145	128	32	32
5	9.64	nd	>256	>256	nd

nd, not determined.

^a Data (K_i) from Charifson et al.¹⁰

strated modest MICs against all three species in the antibacterial assay. The triazolopyridine **4** was ~7-fold less potent against GyrB compared with **3**, however, **4** also showed modest antibacterial activity. Triazolopyridine **5** was approximately 25-fold less active than **3** against the target and did not show any antibacterial activity. The ParE enzyme used in the ATPase assay has a lower specific activity than GyrB, requires more enzyme and therefore more inhibitor to reach an IC₅₀. The ParE inhibitory activity of triazolopyridine **4** was confirmed in this assay. Compared to benzimidazole **2** and novobiocin, compounds **3**, **4** and **5** were significantly less potent but they do lack the additional substituent present in **2**. With the exception of the ParE assay our results for compound **2** were in agreement with data reported by Charifson et al.¹⁰

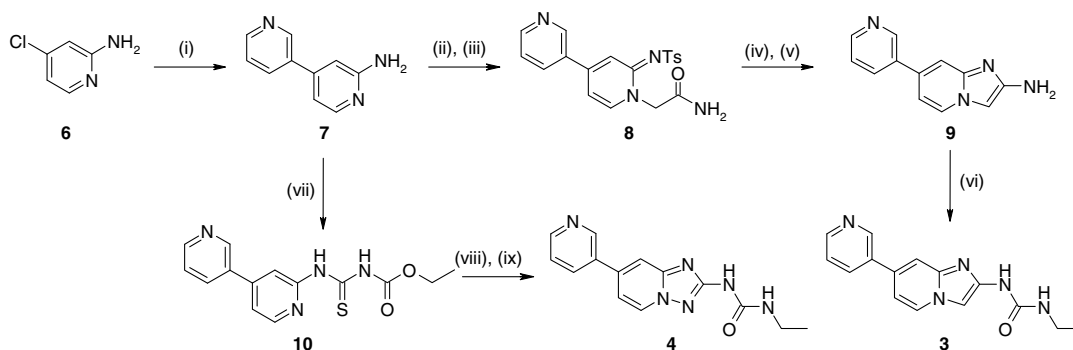
Although the IC₅₀s for all of the scaffolds were below 10 μM, we reasoned that **3** and **4** represented the best opportunities for optimization because they were antibacterial. The lack of antibacterial activity for compound **5** might be related to the higher GyrB IC₅₀ observed for this compound. The higher IC₅₀ for **4** (compared with **3**) might be attributed to the N3 atom in **4** being a weaker H-bond acceptor than the N1 atom in **3** and hence the H-bonding network in the active site of GyrB is weaker.

Further insights from molecular modeling and SAR from Mani et al.⁸ suggested that the 5-position of the new scaffolds would be a good area for SAR exploration to improve the potency. Examination of the chemistry required to access 5-substituted triazolopyridines and imidazopyridines indicated that compound **4** would be more amenable to parallel synthesis.¹⁹ We therefore elected to focus our efforts on the synthesis of 5-substituted triazolopyridines and for this study we continued to fix the 7-substituent as the 3-pyridyl moiety.

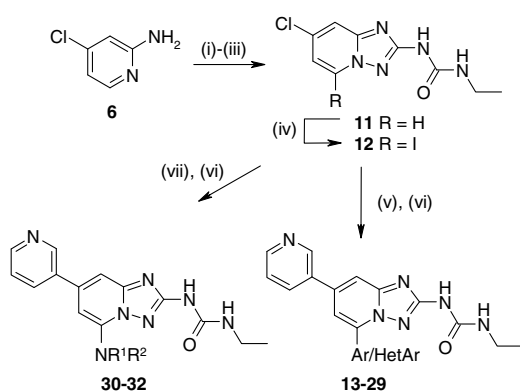
To incorporate functionality into the 5-position of the triazolopyridine scaffold, we modified the original route outlined in Scheme 1 so that the 5-substituent could be introduced during the latter stages of the synthetic sequence. Key to the success of this route was the preparation of **11** on a multi-gram scale. This was achieved in three steps from **6** using an adaptation of the conditions described by Nettekoven et al.¹⁵ as shown in Scheme 2.

From compound **11**, we introduced iodine regioselectively into the 5-position using a modification of a procedure reported by Finkelstein.^{20,21} This provided the iodo intermediate **12** which allowed us to incorporate aromatic (Ar) and heteroaromatic (HetAr) substituents into the 5-position using palladium cross-coupling reactions with boronic acids and trialkyl stannanes. These reactions provided intermediates that were subjected to a second palladium cross-coupling reaction to install the 3-pyridyl moiety in the 7-position to give compounds **13–29**. Alternatively, intermediate **12** was shown to be a substrate for S_NAr or copper-promoted reactions to access N-linked analogues **30–32**, again after a palladium cross-coupling step to introduce the 3-pyridyl group.

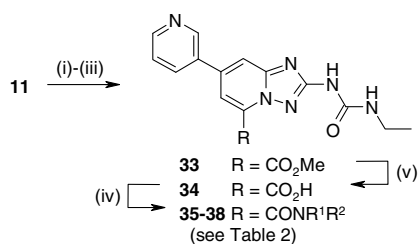
Regioselective deprotonation of intermediate **11** also facilitated the introduction of carboxylic acid derivatives in the 5-position of the triazolopyridine ring related to benzimidazole **2** (Scheme 3).



Scheme 1. Reagents and conditions: (i) 3-pyridyl boronic acid, Pd(dppf)Cl₂, Na₂CO₃, MeCN, μ W, 170 °C, 95%; (ii) TsCl, pyridine, 85 °C, 40%; (iii) ICH₂CONH₂, DIPEA, DMF, rt, 50%; (iv) (CF₃CO)₂O, CH₂Cl₂, 30 °C; (v) K₂CO₃, MeOH, reflux, 20% (2 steps); (vi) a–PhOCOCl, THF, rt; b–EtNH₂, THF, rt, 2% (2 steps); (vii) EtOC(O)NCS, 1,4-dioxane, rt; (viii) NH₂OH·HCl, DIPEA, MeOH:EtOH (1:1), 60 °C; (ix) EtNCO, 1,4-dioxane, 80 °C, 23% (3 steps).



Scheme 2. Reagents and conditions: (i) EtOC(O)NCS, 1,4-dioxane, rt, 95%; (ii) NH₂OH·HCl, DIPEA, MeOH:EtOH (1:1), 60 °C, 72%; (iii) EtNCO, 1,4-dioxane, 80 °C, 84%; (iv) *n*-BuLi (3 equiv), THF, –78 °C, then I₂, 52%; (v) ArB(OH)₂ or HetArB(OH)₂, Pd(dppf)Cl₂, K₃PO₄, MeOH:1,4-dioxane (1:4), 80 °C, ~60%; or RSnBu₃, Pd(PPh₃)₂, CuI, THF, 80 °C, ~35%; (vi) 3-pyridyl boronic acid, Pd(dppf)Cl₂, K₃PO₄, MeOH:1,4-dioxane (1:4), 100 °C, 7–25%; (vii) a–HNR¹R², DMF, 100 °C, ~25%; or b–HNR¹R², CuI, Cs₂CO₃, NMP, 80 °C, ~30%.



Scheme 3. Reagents and conditions: (i) *n*-BuLi (3 equiv), THF, –78 °C, then CO₂; (ii) SOCl₂, MeOH, rt to 75 °C, 18% (over 2 steps); (iii) 3-pyridyl boronic acid, Pd(dppf)Cl₂, K₃PO₄, MeOH:1,4-dioxane (1:4), 100 °C, 39%; (iv) LiOH, 1,4-dioxane, H₂O, rt, 88%; (v) HNR¹R², AlMe₃, 1,4-dioxane, toluene, 45 °C, ~90%.

Thus, treatment of **11** with *n*-butyllithium was followed by a carbon dioxide quench to afford a carboxylic acid (not shown). Esterification of this acid by activation with thionyl chloride and subsequent reaction with methanol was followed by a palladium cross-coupling reaction using 3-pyridyl boronic acid to provide ester **33**. Further functional group manipulation gave access to the parent carboxylic acid **34** or amides, for example, **35–38**.

Biological data for selected compounds synthesized via the routes shown in Schemes 2 and 3 are shown in Table 2.

As indicated by the entries **13–22** in Table 2 a six-membered aromatic ring in the 5-position of the triazolopyridine scaffold pro-

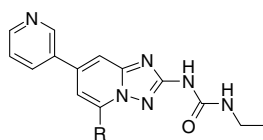
vided compounds with improved IC₅₀s against GyrB compared with the parent unsubstituted compound **4**. The 5-phenyl compound **13** is the most potent (GyrB IC₅₀ 150 nM), although substitutions in the *ortho*-, *meta*- and *para*-positions of the phenyl ring are inhibitors of GyrB. Electron-withdrawing and electron-donating substituents in the phenyl ring provided potent GyrB inhibitors however none of the compounds exhibit antibacterial activity. Compounds **23–26**, containing a six-membered heteroaromatic ring in the 5-position are also active against GyrB (IC₅₀ ~ 1 μ M). With the exception of the 2-pyridyl analogue **23**, which shows modest activity against *E. faecalis*, these compounds are inactive in the antimicrobial screen.

Some highly potent GyrB inhibitors were identified when the substituent in the 5-position of the triazolopyridine scaffold was a five-membered heteroaromatic ring. In particular, thiazole **27** and pyrazole **31** demonstrate IC₅₀s of 42 nM and 54 nM, respectively. Compound **27** shows good antibacterial activity against the Gram-positive organisms with MICs of 1 μ g/ml. The MICs of compound **31** suggests that there is potential for broad-spectrum inhibitors from this class. Of the carboxylic acid derivatives **33–38**, the ethylamide **37** is the most potent GyrB inhibitor with an IC₅₀ of 41 nM. The most potent compounds **27**, **31** and **37** were also screened in the ParE assay and they were all found to be dual inhibitors.

Comparison of substituted triazolopyridines **23**, **24**, **31**, **33** and **36** with the analogous benzimidazoles described by Charifson et al.¹⁰ shows that the benzimidazole scaffold (**2**, **39–42**) leads to more potent enzyme inhibitors (Table 3). One key difference between the scaffolds is the potential for intramolecular H-bonding in the benzimidazole series involving the NH and the R substituent and this might explain some of the observed differences with the enzyme potency SAR, for example, compound **23** versus **39**. Indeed Charifson et al.¹⁰ suggest that coplanarity between the scaffold and the R substituent is particularly important for ParE activity (compound **39** compared with compound **40**). There is clear evidence of divergent antimicrobial SAR between the two scaffolds. Compounds **23**, **24** and **33** have little or no antimicrobial activity but the corresponding benzimidazole analogues **39**, **40** and **2** are antibacterial indicating that the triazolopyridine scaffold is more conservative. The compounds containing a 1-pyrazolyl substituent, **31** and **41** are antibacterial on both scaffolds, although the benzimidazole compound **41** is more potent. Compound **36** is equipotent compared to **42** despite being a less effective enzyme inhibitor on the triazolopyridine scaffold. Further SAR evaluation is necessary in order to optimize the enzyme potency and antibacterial activity on the triazolopyridine scaffold.

The three most potent triazolopyridines, compounds **27**, **31** and **37**, were selected for further characterization. Dual-targeting

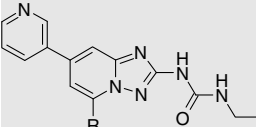
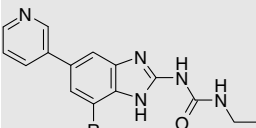
Table 2
GyrB/ParE inhibitory activity and MICs for 5-substituted triazolopyridines



Compound	R	GyrB IC ₅₀ (μM)	ParE IC ₅₀ (μM)	MIC (μg/ml)			
				SA	EF	SP	EC
4	H	2.69	145	128	32	nd	32
13	Ph	0.15	nd	>256	32	128	32
14	2-F Ph	1.52	nd	>256	>256	>256	>256
15	2-OH Ph	0.69	nd	>256	>256	>256	>256
16	3-OMe Ph	0.51	nd	>128	>128	>128	>128
17	4-OMe Ph	0.37	nd	>128	>128	>128	>128
18	3-NHCOMe Ph	1.08	nd	>256	>256	>256	>256
19	3-COMe Ph	1.01	nd	>256	>256	>256	>256
20	3-CONH ₂ Ph	1.01	nd	>256	>256	>256	>256
21	4-OH Ph	0.35	nd	>256	>256	>256	>128
22	3-NMe ₂ Ph	0.84	nd	>256	>256	>256	>256
23		0.89	nd	>256	32	>256	>256
24		0.61	nd	>256	>256	>256	>256
25		1.5	nd	>256	>256	>256	>256
26		0.98	nd	>128	>128	>128	>128
27		0.042	11	1	1	1	>128
28		0.2	nd	>256	8	4	>256
29		0.34	nd	32	8	32	>128
30		1.15	nd	32	32	32	32
31		0.054	25	2	2	2	4
32		1.43	nd	16	16	32	32
33	-CO ₂ Me	1.3	nd	>256	>256	>256	>256
34	-CO ₂ H	2.8	nd	>256	>256	>256	>256
35	-CO ₂ NH ₂	0.64	nd	32	16	16	8
36	-CONHMe	0.64	nd	8	4	8	8
37	-CONHEt	0.041	40	8	4	8	8
38	-CONMe ₂	3.2	nd	256	256	256	256

SA, *S. aureus* ATCC 29213; EF, *E. faecalis* ATCC 29212; SP, *Streptococcus pyogenes* ATCC 51339; EC, *E. coli* ATCC N43; nd, not determined.

Table 3
Head-to-head comparison of the triazolopyridine and benzimidazole scaffolds

Compound	R	GyrB IC ₅₀ ^a (μM)	ParE IC ₅₀ ^a (μM)	SA MIC (μg/ml)	
	23	2-Pyridyl	0.89	nd	>256
	24	3-Pyridyl	0.61	nd	>256
	31	1-Pyrazolyl	0.054	25	2
	33	–CO ₂ Me	1.3	nd	>256
	36	–CONHMe	0.64	nd	8
	39	2-Pyridyl	<0.004	0.014	0.031
	40	3-Pyridyl	0.006	1.3	4
	41	1-Pyrazolyl	<0.004	0.046	0.063
	2	–CO ₂ Me	<0.004	0.035	0.063
	42	–CONHMe	0.005	0.15	16

^a K_i data for compounds **39–42**.

Table 4
Antibacterial activities for compounds **27**, **31** and **37**

Strain	MIC (μg/ml)		
	27	31	37
<i>E. coli</i> ATCC 25922	>128	>128	>128
<i>H. influenzae</i> ATCC 49247	>128	16	16
<i>M. catarrhalis</i> ATCC 25240	0.5	1	2
<i>P. aeruginosa</i> 101021	>128	>128	>128
<i>E. faecalis</i> 1.5604 (VRE)	1	4	4
<i>S. aureus</i> 601055 (MSSA)	1	4	4
<i>S. aureus</i> 43300 (MRSA)	1	4	4
<i>S. aureus</i> ATCC 700698 (MRSA)	0.5	4	2
<i>S. aureus</i> Smith ATCC 19636 (MSSA)	1	4	4
<i>S. pneumoniae</i> ATCC 49619	1	2	4

antibacterials should demonstrate low spontaneous resistance frequencies. No bona fide resistant strains of *S. aureus* at 2×, 4× or 8× the MICs of the compounds were isolated despite multiple attempts. The resistance frequency was estimated to be $<1.8 \times 10^{-9}$, consistent with a dual-targeting inhibitor series. The three compounds demonstrate good activity against a range of pathogenic bacteria including drug-resistant clinical isolates (Table 4) with MICs comparable with the oxazolidinone antibacterial agent linezolid.²² It is interesting to note that all three compounds were ineffective against the *E. coli* strain used in this study. This data, coupled with the data on the efflux pump mutant (shown in Table 2), suggests that compounds in the triazolopyridine series may have reduced permeability as well as some susceptibility to efflux, at least in *E. coli*, however, this has not been investigated further. Overall, the microbiology suggests that this series of compounds would be more suited to a Gram-positive clinical indication.

The mammalian cytotoxicity of **27**, **31** and **37** was evaluated in a HepG2²³ cell assay to test the effect of the compounds on mitochondrial metabolism after 24 h exposure. The IC₅₀ for the compounds were all >64 μg/ml providing a significant window of selectivity for antimicrobial versus cytotoxic activity and indicates that the compounds are not general ATPase inhibitors.

During the course of this work, a patent application describing some of the triazolopyridines described here as antibacterial agents was published.²⁴ In this patent activity against a strain of *Neisseria gonorrhoeae* was reported (e.g. compound **37** MIC of 1 μg/ml) but to our knowledge no additional data on the antimicrobial activity of these compounds has appeared in the literature and the compounds **27** and **31** have not been reported previously.

In conclusion, we have identified an imidazopyridine and a triazolopyridine scaffold which can be functionalized to provide compounds that demonstrate antibacterial activity through inhibition of GyrB/ParE. The triazolopyridine scaffold was selected for further SAR evaluation and compounds with good antibacterial activity, particularly against Gram-positive organisms, have been identified. From our preliminary evaluation it appears that the GyrB IC₅₀s need to be ~500 nM or lower in order to see single digit MICs in the antimicrobial screen. The evaluation of the pharmacokinetics and efficacies of these compounds will be presented in due course.

Acknowledgments

The authors extend their thanks to Dr. Steve Ruston, Dr. Mark Whittaker and Dr. Geoff Lawton for useful discussions during course of this research programme. This work was funded by investments from East Hill Management (Boston, USA). The Prolysis authors declare financial interests.

References and notes

- Mitscher, L. A. *Chem. Rev.* **2005**, *105*, 559.
- Maxwell, A.; Lawson, D. M. *Curr. Top. Med. Chem.* **2003**, *3*, 283.
- Boehm, H.-J.; Boehringer, M.; Bur, D.; Gmuender, H.; Huber, W.; Klaus, W.; Kostrewa, D.; Kuehne, H.; Luebbbers, T.; Meunier-Keller, N.; Mueller, F. J. *Med. Chem.* **2000**, *43*, 2664.
- Oblak, M.; Kotnik, M.; Solmajer, T. *Curr. Med. Chem.* **2007**, *14*, 2033.
- Brino, L.; Urzhumtsev, A.; Mousli, M.; Bronner, C.; Mitschler, A.; Oudet, P.; Moras, D. J. *Biol. Chem.* **2000**, *275*, 9468.
- Dale, G. E.; Kostrewa, D.; Gsell, B.; Stieger, M.; D'Arcy, A. *Acta. Crystallogr.* **1999**, *D55*, 1626.
- Tanitime, A.; Oyamada, Y.; Ofuji, K.; Fujimoto, M.; Iwai, N.; Hiyama, Y.; Suzuki, K.; Ito, H.; Terauchi, H.; Kawasaki, M.; Nagai, K.; Wachi, M.; Yamagishi, J.-I. *J. Med. Chem.* **2004**, *47*, 3693.
- Mani, N.; Gross, C. H.; Parsons, J. D.; Hanzelka, B.; Müh, U.; Mullin, S.; Liao, Y.; Grillot, A.-L.; Stamos, D.; Charifson, P. S.; Grossman, T. H. *Antimicrob. Agents Chemother.* **2006**, *50*, 1228.
- Grossman, T. H.; Bartels, D. J.; Mullin, S.; Gross, C. H.; Parsons, J. D.; Liao, Y.; Grillot, A.-L.; Stamos, D.; Olson, E. R.; Charifson, P. S.; Mani, N. *Antimicrob. Agents Chemother.* **2007**, *51*, 657.
- Charifson, P. S.; Grillot, A.-L.; Grossman, T. H.; Parsons, J. D.; Badia, M.; Bellon, S.; Deinger, D. D.; Drumm, J. E.; Gross, C. H.; LeTiran, A.; Liao, Y.; Mani, N.; Nicolau, D. P.; Perola, E.; Ronkin, S.; Shannon, D.; Swenson, L. L.; Tang, Q.; Tessier, P. R.; Tian, S. K.; Trudeau, M.; Wang, T.; Wei, Y.; Zhang, H.; Stamos, D. J. *Med. Chem.* **2008**, *51*, 5243.
- Meigh, J.-P.; Alvarez, M.; Joule, J. A. *J. Chem. Soc., Perkin Trans. 1* **2001**, 1202.
- Hamdouchi, C.; de Blas, J.; del Prado, M.; Gruber, J.; Heinz, B. A.; Vance, L. J. *Med. Chem.* **1999**, *42*, 50.
- All compounds described in this manuscript were characterized by LC-MS and ¹H NMR.
- The yield for step (vi) of the reaction sequence illustrated in Scheme 1 represents the yield from one unoptimised reaction.
- Nettekoven, M.; Püllmann, B.; Schmitt, S. *Synthesis* **2003**, 1649.

16. Gyrase B and ParE convert ATP into ADP and inorganic phosphate. The released phosphate can be detected by the addition of malachite green solution and measured by monitoring the increase in absorbance at 600 nm. The GyrB ATPase assay is carried out in a buffer containing 12.8 nM Gyrase enzyme (A_2B_2 complex from *E. coli*), 0.08 mg/mL ssDNA, 35 mM Tris, pH 7.5, 24 mM KCl, 2 mM $MgCl_2$, 6.5% glycerol, 2 mM DDT, 1.8 mM spermidine, 0.1 mg/mL BSA, and 5% DMSO solution containing the inhibitor in a total volume of 25 μ l. The reaction is started by adding ATP to a final concentration of 1 mM and allowed to incubate at 30 °C for 60 min. The reaction is stopped by adding 200 μ l of malachite green solution (0.034% malachite green, 10 mM ammonium molybdate, 1 M HCl, 3.4% ethanol, 0.01% Tween 20). Colour is allowed to develop for 5 min and the absorbance at 600 nm is measured spectrophotometrically. The IC_{50} values are determined from the absorbance readings using no compound and no enzyme controls. The ParE assay is performed in a buffer containing 43 nM TopoIV enzyme from *E. coli*, 10 μ g/mL ssDNA, 100 mM Tris, pH 7.5, 20 mM KCl, 6 mM $MgCl_2$, 10 mM DDT, 0.1 mg/mL BSA, and 5% DMSO solution containing the inhibitor with 0.5 mM ATP added to start the reaction.
17. Compounds were tested for antimicrobial activity by susceptibility testing in liquid or on solid media. MICs for compounds against each strain were determined by the broth microdilution or agar dilution method according to the guidelines of the Clinical Laboratories and Standards Institute described in CLSI Methods for Antimicrobial Susceptibility Testing of Anaerobic Bacteria Approved Standard, 6th ed., Document M11-A6, Vol. 24(2), January 2004 and CLSI Methods for Dilution Antimicrobial Susceptibility Tests for Bacteria That Grow Aerobically; Approved Standard, 7th ed.: M7-A7E, Vol. 26(2), January 2006.
18. MICs estimated in triplicate once. Activity of compounds confirmed. For compounds **27**, **31** and **37** $n > 10$.
19. During the course of our optimization programme on the triazolopyridine series we became aware of a patent that reported imidazopyridines and imidazopyrimidines as antibacterial agents: Sciotti, R. J.; Starr, J. T.; Richardson, C.; Rewcastle, G. W.; Palmer, B. D.; Sutherland, H. S.; Spicer, J. A.; Chen, H. Int. Pat. Appl. WO 2005089763, 2005.
20. Finkelstein, B. J. *Org. Chem.* **1992**, *57*, 5538.
21. Three equivalents of *n*-butyllithium were critical to the success of this reaction. Experimental procedure: To a solution of 1-(7-chloro-[1,2,4]triazolo[1,5-*a*]pyridin-2-yl)-3-ethyl-urea **11** (200 mg, 0.834 mmol) in THF (8 mL) at –78 °C was added *n*-BuLi (1.5 mL of a 1.67 M solution, 2.5 mmol) dropwise. The resulting mixture was stirred at –78 °C for 5 min and then warmed to 0 °C where it was maintained for 1 h. After this time, the solution was re-cooled to –78 °C and iodine (648 mg, 2.5 mmol) as a solution in THF (4 mL) was introduced dropwise. The reaction mixture was stirred for 2 h at –78 °C before sat. NH_4Cl (4 mL) was added followed by sat. sodium thiosulfate (1 mL). The solution was extracted with dichloromethane (3 \times) and the combined organic extracts were dried (Na_2SO_4), filtered and concentrated in vacuo to reveal a yellow solid. This solid was purified by chromatography on silica, using 1–2% MeOH/dichloromethane as the eluent, to provide 1-(7-chloro-5-iodo-[1,2,4]triazolo[1,5-*a*]pyridin-2-yl)-3-ethyl-urea **12** as a yellow solid (160 mg, 52%). MS: m/z 366 $[M+H]^+$. 1H NMR (DMSO): δ = 10.16 (s, 1H), 8.16 (t, J = 5 Hz, 1H), 7.97 (d, J = 2 Hz, 1H), 7.86 (d, J = 2 Hz, 1H), 3.34 (m, J = 7, 5 Hz, 2H), 1.24 (t, J = 7 Hz, 3H).
22. Barbachyn, M. R.; Ford, C. W. *Angew. Chem. Int. Ed.* **2003**, *42*, 2010.
23. HepG2 cytotoxicity assays were performed by Precos Ltd, University of Nottingham, UK. Briefly, HepG2 cells were incubated with compound for 48 hours. Mitochondrial dehydrogenase activity was measured.
24. Butler, D. C. D.; Chen, H.; Hegde, V. R.; Limberakis, C.; Rasne, R. M.; Sciotti, R. J.; Starr, J. T. Int. Pat. Appl. WO2006038116, 2006